

Dynamics of magnetostatically coupled vortices in magnetic nanodisks

Junya Shibata, Kunji Shigeto, and Yoshichika Otani
 FRS, RIKEN, 2-1 Hirosawa, Wako, Saitama 351-0198, Japan
 (Received 27 December 2002; published 5 June 2003)

The dynamics of magnetostatically coupled vortices in two nanodisks is here investigated analytically and numerically. The rigid vortex model is employed to calculate the magnetostatic interaction between the nanodisks. We use Thiele's equation where collective degrees of freedom describe the motion of each vortex core. We find that there are eigenfrequencies of circular vortex core motion around the disk center, which depend on the core polarizations of the vortices. We also obtain the energy absorption rate of the system when subjected to an oscillating in-plane magnetic field. Finally, we can draw an analogy between this vortex system and a van der Waals diatomic molecule.

DOI: 10.1103/PhysRevB.67.224404

PACS number(s): 75.40.Gb, 75.25.+z, 75.75.+a

I. INTRODUCTION

Recent developments in nanofabrication and precise measurement techniques have enabled us to study laterally confined nanoscale magnetic structures. We are thus gaining insight on nanomagnetism. Among these research activities, investigations on magnetic vortices, stabilized in circular nanodisks, have drawn much attention both experimentally¹⁻⁷ and theoretically.⁸⁻¹⁰

A magnetic vortex appears as a stable magnetic state resulting from competition between the exchange, magnetostatic, and magnetic anisotropy energies, whose magnitude depend on the size and the sample geometry.^{11,12} Hence the important parameters in the system include the disk radius R , the disk thickness L , and the exchange length $R_E = \sqrt{A/\mu_0 M_s^{-1}}$, where A is the exchange stiffness constant, and M_s is the saturation magnetization. The vortex state is well stabilized in the nanodisks when $g \equiv L/R \ll 1$ and $R, L \gg R_E$.

There are theoretical works on the dynamics of the single off-centered vortex.^{13,14} The vortex core was shown to exhibit circular motion around the disk center where the rotational direction depends on the sign of the core polarization. However, the dynamical property of coupled vortices has not been studied. In this paper, we present results on the dynamics of coupled vortices in two nanodisks. The magnetostatic interaction between two closely spaced disks was found to play an important role in determining the dynamics of vortices. In addition, we can draw an analogy between the dynamical system of two vortices and a diatomic molecule with the van der Waals bonding induced by the dipole interaction.

A magnetic vortex is a nonlinear spin configuration, and a kind of topological soliton.¹⁵ Static properties of such a vortex are determined by the following topological quantities: the vorticity ($q = \pm 1, \pm 2, \dots$), the polarization ($p = \pm 1$), and the chirality ($C = \pm 1$). The vorticity q describes the number of windings of the magnetization vector projected on the order-parameter space. The plus or minus sign in q corresponds to the counterclockwise or clockwise rotation of the magnetization. In this paper, we only consider the $q = 1$ case. The polarization p refers to the magnetization direction of the vortex core. The up or down magnetization along the cylinder axis of the vortex core corresponds to $p = 1$ or

-1 , respectively. The chirality C refers to the counterclockwise ($C = 1$) or the clockwise ($C = -1$) rotational direction of the magnetization in the dot plane.

II. ANALYTICAL CALCULATIONS

A. Interaction energy of two-coupled vortices

Let us discuss the dynamics of magnetostatically coupled vortices. As shown in Fig. 1, the vortices are separated along the x axis by a distance between disk centers defined as $D \equiv dR$. When each vortex core is shifted from its disk center, magnetic charges $\sigma(\phi_i)$ ($i = 1, 2$) emerge on the side surface of the disk. In the rigid vortex model,⁹ these charges are given by

$$\sigma(\phi_i) = -C_i \frac{a_{ix} \sin \phi_i - a_{iy} \cos \phi_i}{\sqrt{1 + |\mathbf{a}_i|^2 - 2(a_{ix} \cos \phi_i + a_{iy} \sin \phi_i)}}, \quad (1)$$

where $\mathbf{a}_i \equiv (a_{ix}, a_{iy}) \equiv (A_{ix}, A_{iy})/R$ is the dimensionless position of the i th vortex center. Using Eq. (1), the magnetostatic energy between the side surfaces of two disks can be expressed as

$$\begin{aligned} W_{\text{int}}(\mathbf{a}_1, \mathbf{a}_2) &= \frac{\mu_0 M_s^2 R^3}{8\pi} \int \frac{dz_1 dz_2 d\phi_1 d\phi_2 \sigma(\phi_1) \sigma(\phi_2)}{K(\phi_1, z_1, \phi_2, z_2)} \\ &= C_1 C_2 (\eta_x a_{1x} a_{2x} - \eta_y a_{1y} a_{2y}) + \mathcal{O}(|a|^3), \quad (2) \end{aligned}$$

where

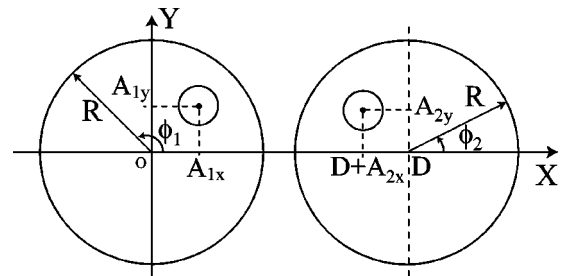


FIG. 1. Schematic illustration of two disks with vortices. The coordinates of each vortex center are denoted by (A_{1x}, A_{1y}) and $(D + A_{2x}, A_{2y})$, respectively.

$$\eta_x = \frac{\mu_0 M_s^2 R^3}{8\pi} \int \frac{dz_1 dz_2 d\phi_1 d\phi_2 \sin \phi_1 \sin \phi_2}{K(\phi_1, z_1, \phi_2, z_2)}, \quad (3a)$$

$$\eta_y = -\frac{\mu_0 M_s^2 R^3}{8\pi} \int \frac{dz_1 dz_2 d\phi_1 d\phi_2 \cos \phi_1 \cos \phi_2}{K(\phi_1, z_1, \phi_2, z_2)}, \quad (3b)$$

with $K(\phi_1, z_1, \phi_2, z_2) = (d^2 + 2d(\cos \phi_2 - \cos \phi_1) + 2 - 2 \cos(\phi_2 - \phi_1) + (z_2 - z_1)^2)^{1/2}$. The integration of Eq. (2) runs from 0 to g in z_1, z_2 and from 0 to 2π in ϕ_1, ϕ_2 . Here we assume that the vortex displacement $|\mathbf{a}_i|$ is much smaller than the disk radius R and expand the above energy in a series on $|\mathbf{a}_i|$, up to second order. Since the core radius of the vortex is small enough compared with the disk radius R , the interactions between the charge distribution on the top and bottom surfaces of two disks are negligible. By adding the magnetostatic energy in Eq. (2) to the energy given in Ref. 9, the total energy of two off-centered vortices in two nearby disks is given by

$$W(\mathbf{a}_1, \mathbf{a}_2) = \sum_{i=1}^2 [W_{\text{es}}(|\mathbf{a}_i|) + W_Z(\mathbf{a}_i)] + W_{\text{int}}(\mathbf{a}_1, \mathbf{a}_2). \quad (4)$$

Here, $W_{\text{es}}(|\mathbf{a}_i|) = \kappa |\mathbf{a}_i|^2 / 2 + \mathcal{O}(|\mathbf{a}_i|^4)$ is a sum of the exchange and magnetostatic energies of a single off-centered vortex; $\kappa = \mu_0 M_s^2 V [F_1(g) - (R_E/R)^2]$, $F_1(g) = \int_0^\infty dk f(kg) J_1^2(k)/k$, $f(x) = 1 - (1 - e^{-x})/x$, V is the volume of the disk, and $J_1(x)$ is the Bessel's function of the first order. On the other hand, $W_Z(\mathbf{a}_i) = -C_i \mu_0 M_s V [H_x(t) a_{iy} - H_y(t) a_{ix}] + (|\mathbf{a}_i|^3)$ is the Zeeman energy of the in-plane external magnetic field $\mathbf{H}_{\text{ex}} = H_x(t) \mathbf{e}_x + H_y(t) \mathbf{e}_y$.

B. Dynamics of two-coupled vortices

The investigation of the dynamics of vortices is based on Thiele's equation.^{16,17} This equation is described by collective degrees of freedom of magnetic domains, which is derived from the Landau-Lifshitz-Gilbert equation. Conditions for applying Thiele's equation are the constant saturation magnetization M_s and the vortex core displacement without distortion. In the case of a magnetic vortex, these collective degrees of freedom are the core position of the vortex. Here we consider the displacement parameters \mathbf{A}_i to be the dynamical variables $\mathbf{A}_i(t)$. Using these variables, the equation of motion of the vortex center can be written as

$$\mathbf{G}_i \times \frac{d\mathbf{A}_i(t)}{dt} = \frac{\partial W(\mathbf{a}_1(t), \mathbf{a}_2(t))}{\partial \mathbf{A}_i(t)} - \tilde{\mathbf{D}}_i \cdot \frac{d\mathbf{A}_i(t)}{dt}, \quad (5)$$

where \mathbf{G}_i and $\tilde{\mathbf{D}}_i$ are the gyrovector and the dissipation dyadic. In the rigid vortex model, they are calculated as

$$\mathbf{G}_i = -\frac{2\pi p_i L \mu_0 M_s}{\gamma} \mathbf{e}_z, \quad (6a)$$

$$\tilde{\mathbf{D}}_i = -\frac{2\pi L \alpha \mu_0 M_s}{\gamma} (\mathbf{e}_x \cdot \mathbf{e}_x + \mathbf{e}_y \cdot \mathbf{e}_y), \quad (6b)$$

where γ is the gyromagnetic ratio, and α is the nondimensional damping parameter. The set of equations above is

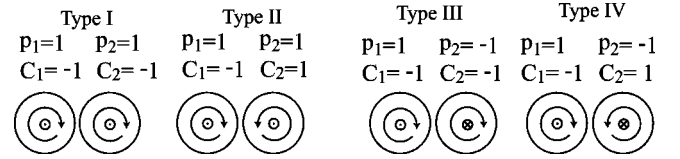


FIG. 2. Schematic diagram of vortices for various combinations of polarizations p and chiralities C . A circle with a dot and a circle with cross represent polarizations for $p = +1$ and -1 , respectively. Circular arrows represent the chiralities.

equal to two-dimensional damped coupled oscillations in a time-dependent external field. There are topologically different types of the two-vortex system. They are classified into four types labeled “type I,” “type II,” “type III,” and “type IV,” as in Fig. 2, according to different combinations of polarizations and chiralities of vortices: $(p_1, p_2, C_1, C_2) = (1, 1, -1, -1), (1, 1, -1, 1), (1, -1, -1, -1), (1, -1, -1, 1)$. All the possible combinations belong to one of these types. From the above set of Eqs. (5), we obtain eigenfrequencies which depend on the polarizations p_i of vortices:

$$\omega_{p_1, p_2} = \frac{\omega_0}{1 + \alpha^2} \times \sqrt{(1 + p_1 p_2 \lambda_x)(1 - \lambda_y) - \alpha^2 \left(\frac{p_1 p_2 \lambda_x + \lambda_y}{2} \right)^2}, \quad (7a)$$

$$\omega_{p_1, p_2}^* = \frac{\omega_0}{1 + \alpha^2} \times \sqrt{(1 - p_1 p_2 \lambda_x)(1 + \lambda_y) - \alpha^2 \left(\frac{p_1 p_2 \lambda_x + \lambda_y}{2} \right)^2}, \quad (7b)$$

where $\omega_0 = \kappa / (R^2 |\mathbf{G}|) = \gamma M_s [F_1(g) - (R_E/R)^2] / 2$ is the characteristic frequency of the circulating single vortex, and $\lambda_i \equiv \eta_i / \kappa$ ($i = x, y$). The eigenmotions with their eigenfrequencies $\omega_{1,1}, \omega_{1,-1}$ for each type can be excited with an initial condition on Eqs. (5) as $(A_{1x}(0), A_{1y}(0), A_{2x}(0), A_{2y}(0)) = (0, C_1 \delta HR, 0, C_2 \delta HR)$. Here H is a uniform external magnetic field in the x direction to set initially each vortex center on an off-centered position, and δ is the appropriate constant determined by the steady condition of Eqs. (5). After removing the magnetic field H , both vortex cores coherently rotate around the disk centers with the normal-mode frequencies $\omega_{1,1}$ for types I and II and $\omega_{1,-1}$ for types III and IV, and relax back to the disk centers in the absence of a time-dependent external magnetic field. On the other hand, if we impose the initial condition on Eqs. (5) as $(A_{1x}(0), A_{1y}(0), A_{2x}(0), A_{2y}(0)) = (0, C_1 \delta HR, 0, -C_2 \delta HR)$, the other normal modes $\omega_{1,1}^*, \omega_{1,-1}^*$ are excited. This initial condition corresponds to the case where a spatially modulated magnetic field is initially applied along the positive x direction on a boundary between centers of the two disks. After all, vortex cores coherently rotate in the same direction

for types I and II ($p_1=1, p_2=1$), and in the opposite direction for types III and IV ($p_1=1, p_2=-1$).

We now consider the effect of the periodically oscillating external magnetic field, $\mathbf{H}_{\text{ex}}(t)=H_{\text{ex}}(t)\mathbf{e}_x$, with $H_{\text{ex}}(t)=H_{\text{ex}}\cos(\Omega t)$, on the motion of the vortices. When the frequency Ω is close to the resonant frequency Ω_{p_1, p_2}^R , the vortex core continues to rotate around the disk center, while absorbing the external energy. From Eq. (5), the energy absorption rate per unit time is given by

$$I(\alpha, \Omega/\omega_0) = -\sum_{i=1}^2 \frac{\overline{d\mathbf{A}_i(t)}}{dt} \cdot \vec{\mathbf{D}}_i \cdot \frac{d\mathbf{A}_i(t)}{dt}, \quad (8)$$

where the over line means the time average over a period. The above equation can be calculated as

$$I(\alpha, \Omega/\omega_0) = \gamma \frac{\mu_0 M_s V}{2} H_{\text{ex}}^2 f(\alpha, \Omega/\omega_0), \quad (9)$$

with

$$f(\alpha, x) = \frac{2\alpha\{\beta_1^2 + \beta_3^2 x^2\}x^2}{\beta_1^2 \beta_2^2 + \{\alpha^2(\beta_1^2 + \beta_2^2) - 2\beta_1 \beta_2\}x^2 + \beta_3^4 x^4}, \quad (10)$$

where $\beta_1 = 1 + p_1 p_2 \lambda_x$, $\beta_2 = 1 - \lambda_y$, and $\beta_3^2 = 1 + \alpha^2$. The energy absorption rate $I(\alpha, \Omega/\omega_0)$ is proportional to the square of the amplitude of magnetic field H_{ex} , and depends on the polarizations p_i of the vortices. From Eq. (10), the resonant frequency Ω_{p_1, p_2}^R is given by

$$\Omega_{p_1, p_2}^R = \omega_0 \sqrt{\frac{\beta_1^2 \beta_2}{\beta_3(\beta_1 + \beta_2) - \beta_3^2 \beta_2}}. \quad (11)$$

Strictly speaking, the resonant frequency Ω_{p_1, p_2}^R is not the same as the eigenfrequency in Eq. (7) because the pumping magnetic field $H_{\text{ex}}(t)$ is a linearly polarized field. If appropriate circularly polarized magnetic fields are applied to the rotating vortices system, the resonant frequency and the eigenfrequency coincide well with each other. In the case of a weak damping of $\alpha \ll 1$, both frequencies obtained from Eqs. (7a) and (11) are in good agreement up to the leading order $\mathcal{O}(\alpha^0)$.

III. NUMERICAL CALCULATIONS

Here, we evaluate numerical values on the basis of results obtained from the analytical calculation and the numerical simulation. The computational material parameters are typical for permalloy; the saturation magnetization $M_s = 8.60 \times 10^5$ A/m, the exchange stiffness constant $A = 1.3 \times 10^{-11}$ J/m, the gyromagnetic constant $\gamma = 2.2 \times 10^5$ m/A s, the disk radius $R = 0.1 \mu\text{m}$, and the disk thickness $L = 20$ nm.

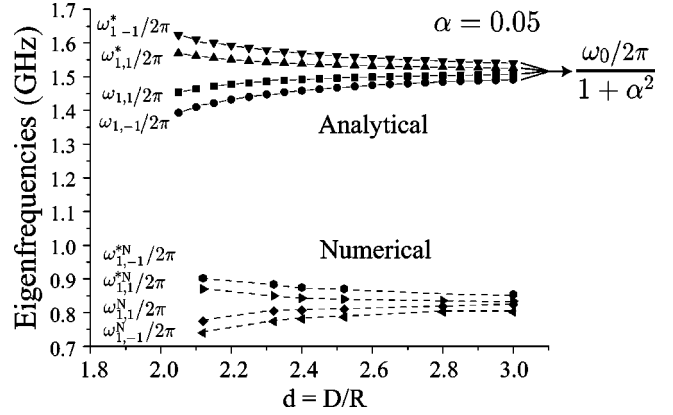


FIG. 3. Analytically estimated eigenfrequencies (ω_{p_1, p_2}^* , ω_{p_1, p_2}^{*N}) and numerically estimated eigenfrequencies (ω_{p_1, p_2}^N , ω_{p_1, p_2}^{*N}) as a function of the nondimensional distance $d = D/R$ for a weak damping $\alpha = 0.05$.

A. Numerical evaluation of analytical results

The characteristic resonant frequency ω_0 of an isolated vortex with no damping can be estimated as $\omega_0 = 1.53$ GHz. Numerically integrating Eq. (3a) then yields eigenfrequencies for the coupled vortices. Figure 3 shows eigenfrequencies obtained for various combinations of polarizations p_i and initial magnetic configurations as a function of nondimensional separating distance d for a sufficiently weak damping $\alpha = 0.05$. In the case of large distance $d \gg 1$, all eigenfrequencies are degenerate at the eigenfrequency ω_0 of the isolated vortex. When the separating distance d is decreased, the degeneracy is removed, and the eigenfrequencies are split into four frequency levels, two higher ($\omega_{1,1}^*$, $\omega_{1,-1}^*$) and two lower ($\omega_{1,1}^N$, $\omega_{1,-1}^N$) than ω_0 , for the isolated vortex case. It should be noted here that the chirality of the vortex has nothing to do with the rotational direction determined only by the core polarization. For types I and II with $\omega_{1,1}$, the average magnetization vectors in the coupled disks always align parallel to each other during rotation because of the same core polarization, $p_1 = p_2 = 1$. On the other hand, for types III and IV, with $\omega_{1,-1}$, the average magnetization vectors rotate opposite to each other because of different core polarizations, $p_1 = -p_2 = 1$, resulting in an anti-parallel configuration of the magnetization vectors appearing during rotation. This may diminish the magnetostatic interaction energy, resulting in the lowest frequency $\omega_{1,-1}$. In the same manner, it can be understood that different initial conditions and magnetic vector configurations lead to the highest $\omega_{1,-1}^*$ and the second highest $\omega_{1,1}^*$. All the above results draw an analogy between the dynamical vortices system and a molecular system with the van der Waals interaction induced by dipole-dipole interaction.

Here, we estimate the binding energy of the system as the time-averaged magnetostatic interaction energy $\overline{W}_{\text{int}}$ vs separating distance d in the case of lower frequencies motion and no damping. Figure 4 shows that this interaction energy varies proportional to the minus sixth power of the separating distance d . The energy thus behaves similarly to that of the van der Waals molecular system when two atoms do not overlap each other.

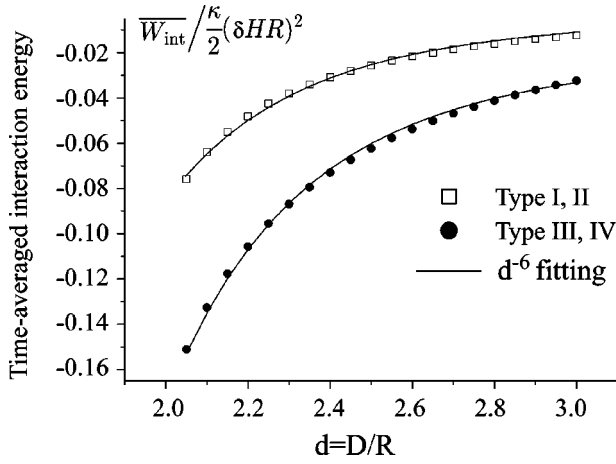


FIG. 4. The time-averaged magnetostatic interaction energy $\overline{W}_{\text{int}}$ as a function of the separating distance d without damping. This illustrates van der Waals interaction.

Figure 5 shows the energy absorption rate $I(\alpha, \Omega/\omega_0)$, in units of $\gamma\mu_0 M_s V H_{\text{ex}}^2/2 = 2.38 \times 10^{-9}$ J/s, as a function of the reduced frequency Ω/ω_0 for types I and II with $p_1 = p_2 = 1$. For types III and IV, the absorption curves are almost the same as those for types I and II. Notice that the resonant frequencies Ω_{p_1, p_2}^R for various distances d lie on the lower eigenfrequencies in Fig. 3. Therefore a spatially uniform magnetic field $H_{\text{ex}}(t)$ may excite the lower eigenfrequencies ($\omega_{1,1}, \omega_{1,-1}$), whereas the higher frequencies ($\omega_{1,1}^*, \omega_{1,-1}^*$) may only be excited by a spatially modulated magnetic field.

B. Micromagnetic calculation

For comparison, the dynamical behavior of the coupled vortex was evaluated using the Object-Oriented Micromagnetic Framework (OOMMF) (Ref. 18) software. We took a cell size of 4.0 nm. Figure 6 shows time evolution of magnetization components $M_x(t)$ and $M_y(t)$ for various combinations of polarizations and chiralities with $d=2.4$. As an initial condition, we set the state where both vortex cores were shifted along the y axis from the center by applying a uniform magnetic field of

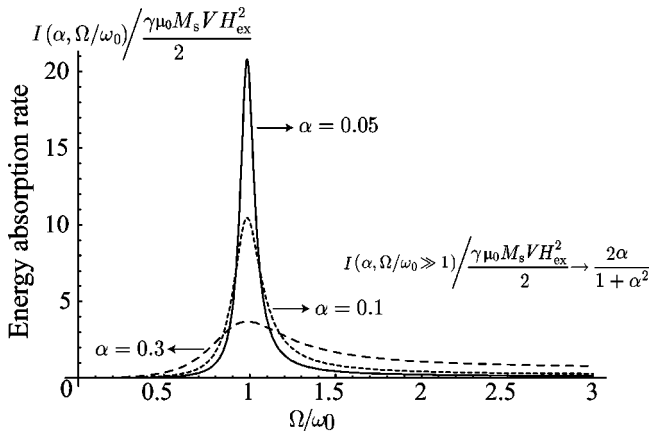


FIG. 5. The energy absorption rate $I(\alpha, \Omega/\omega_0)$ as a function of Ω/ω_0 in the case of type-I and -II coupled vortex system. We take the nondimensional distance $d=2.4$.

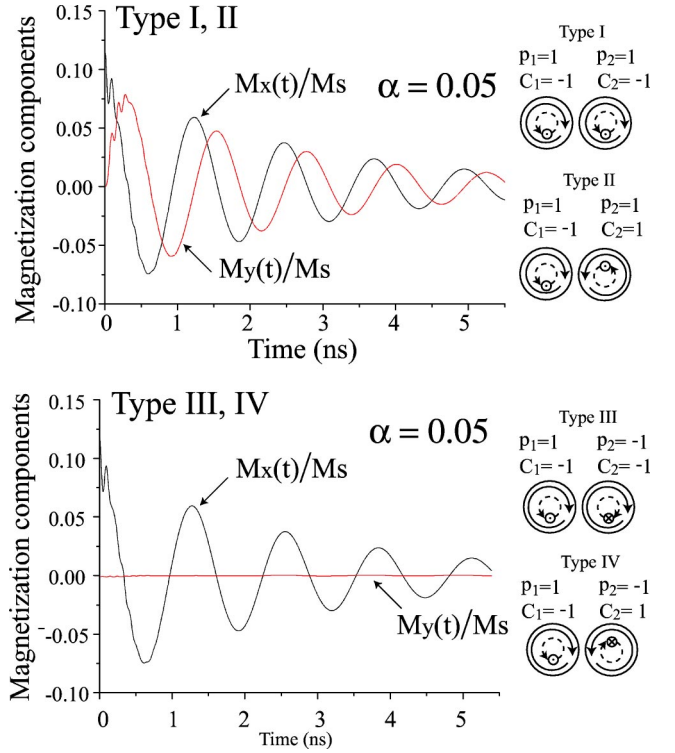


FIG. 6. Time evolution of magnetization components $M_x(t)$ and $M_y(t)$ for various combinations of polarizations and chiralities. We take the damping parameter $\alpha=0.05$, the nondimensional separating distance $d=2.4$. A circular arrow of dashed line represents a rotational direction of vortex motion.

10 mT in the positive x direction. Time evolution of the components $M_x(t)$ and $M_y(t)$ were then simulated after removing the magnetic field. As shown in Fig. 6, the components $M_x(t)$ and $M_y(t)$ for types I and II exhibit damped oscillations, corresponding to the fact that both vortices coherently rotate in same direction and relax back to the disk centers. For types III and IV, the component $M_x(t)$ exhibits damped oscillation, while the component $M_y(t)$ stays constant. This implies that vortices rotate opposite to each other, to cancel the net $M_y(t)$ component, supporting the analytically obtained results in the above discussion.

The higher $\omega_{1,1}^{*N}$ and $\omega_{1,-1}^{*N}$ as well as the lower $\omega_{1,1}^N$ and $\omega_{1,-1}^N$ eigenfrequencies are estimated as a function of the separating distance d from micromagnetic calculations as shown in Fig. 3. The tendency of the variation is in good agreement with the analytically obtained results although the numerical values of the eigenfrequencies and the difference between the higher and the lower eigenfrequencies $\omega_{p_1, p_2}^{*N} - \omega_{p_1, p_2}^N$ are smaller than the analytical ones. This has been pointed out in Ref. 13, where the authors separately estimated the eigenfrequency ω_0 on the basis of rigid vortex and two vortex “side charges free” models.¹⁰ Although the latter model is in good quantitative agreement with the micromagnetic calculation of the eigenfrequency ω_0 , it is not suitable for the coupled vortices system because the vortex structure of this model always has no side surface charges responsible for the coupling. Hence a more precise model is needed to

describe quantitatively the dynamics of coupled vortices system, though the rigid vortex model is useful for a qualitative understanding.

IV. SUMMARY AND DISCUSSION

In conclusion, we investigated in detail the dynamics of magnetostatically coupled vortices in magnetic circular nanodisks, both analytically and numerically. It was shown that coupled vortices coherently rotate around the disk centers with circular eigenfrequencies, which depend on the polarizations of the vortices. Remarkably, the chiralities of the vortices do not influence the dynamics of vortices. We showed that these lower eigenfrequencies ($\omega_{1,1}, \omega_{1,-1}$) for each type of coupled vortex system can be excited by a time-dependent periodically oscillating external magnetic field. It was found that the time-averaged magnetostatic interaction

energy varies as the minus sixth power of the separating distance d . Hence these results can draw an analogy between the dynamical system of coupled nearby vortices and a diatomic molecule with the van der Waals bonding induced by the dipolar interaction. Magnetic charges on the side surfaces of the off-centered nearby vortices induce the magnetic dipole-dipole interaction. Furthermore, without difficulty, our investigation can be extended to an array of magnetostatically coupled $N \times N$ dots, and it is expected that such a system forms a band structure. Finally, we hope that our investigation will open up the possibility of studying two-dimensional artificial crystals in magnetic vortex systems.

ACKNOWLEDGMENT

We are grateful to F. Nori for many useful discussions.

-
- ¹C. Miramond, C. Fermon, F. Rousseaux, D. Decanini, and F. Carcenac, *J. Magn. Magn. Mater.* **165**, 500 (1997).
²R. P. Cowburn, D. K. Koltsov, A. O. Adeyeye, M. E. Welland, and D. M. Tricker, *Phys. Rev. Lett.* **83**, 1042 (1999).
³A. Fernandez and C. C. Cerjan, *J. Appl. Phys.* **87**, 1395 (2000).
⁴T. Shinjo, T. Okuno, R. Hassdorf, K. Shigeto, and T. Ono, *Science (Washington, DC, U.S.)* **289**, 930 (2000).
⁵J. Raabe, R. Pulwey, R. Sattler, T. Schweinböck, J. Zweck, and D. Weiss, *J. Appl. Phys.* **88**, 4437 (2000).
⁶M. Schneider, H. Hoffmann, and J. Zweck, *Appl. Phys. Lett.* **77**, 2909 (2000).
⁷V. Novosad, K. Yu. Guslienko, H. Shima, Y. Otani, S. G. Kim, K. Fukamichi, N. Kikuchi, O. Kitakami, and Y. Shimada, *Phys. Rev. B* **65**, 060 402 (2002).
⁸K. Yu. Guslienko and K. L. Metlov, *Phys. Rev. B* **63**, 100403 (2001).
⁹K. Yu. Guslienko, V. Novosad, Y. Otani, H. Shima, and K. Fukamichi, *Appl. Phys. Lett.* **78**, 3848 (2001); *Phys. Rev. B* **65**, 024414 (2002).
¹⁰K. L. Metlov and K. Y. Guslienko, *J. Magn. Magn. Mater.* **242-245**, 1015 (2002).
¹¹A. Aharoni, *J. Appl. Phys.* **68**, 2892 (1990).
¹²N. A. Usov and S. E. Peschany, *J. Magn. Magn. Mater.* **118**, L290 (1993).
¹³K. Yu. Guslienko, B. A. Ivanov, V. Novosad, Y. Otani, H. Shima, and K. Fukamichi, *J. Appl. Phys.* **91**, 8037 (2002).
¹⁴N. A. Usov and L. G. Kurkina, *J. Magn. Magn. Mater.* **242-245**, 1005 (2002).
¹⁵A. M. Kosevich, B. A. Ivanov, and A. S. Kovalev, *Phys. Rep.* **194**, 117 (1990).
¹⁶A. A. Thiele, *Phys. Rev. Lett.* **30**, 230 (1973).
¹⁷D. L. Huber, *Phys. Rev. B* **26**, 3758 (1982).
¹⁸M. J. Donahue and D. G. Porter, *OOMMF User's Guide, Version 1.0*, Interagency Report NIST IR 6376, Gaithersburg, MD, 1999.